

FERMILAB-PUB-98/383-A

UF-IFT-HEP-98-34

Original: December 1998

Revised: May 1999

A NEW LIMIT ON THE ANTIPROTON LIFETIME

Stephen H. Geer

Fermi National Accelerator Laboratory

and

Dallas C. Kennedy

University of Florida

ABSTRACT

Measurements of the cosmic ray \bar{p}/p ratio are compared to predictions from an inhomogeneous leaky disk model of \bar{p} production and propagation within the Galaxy, combined with a calculation of the modulation of the interstellar cosmic ray spectra as the particles propagate through the heliosphere to the Earth. The predictions agree with the observed \bar{p}/p spectrum. Adding a finite \bar{p} lifetime to the model, we obtain the limit $\tau_{\bar{p}} > 0.8$ Myr (90% C.L.).

Subject headings: elementary particles — ISM: cosmic rays — Sun: solar wind

Submitted to **the Astrophysical Journal**

In recent years the presence of antiprotons (\bar{p} 's) in the cosmic ray (CR) flux incident upon the Earth has been firmly established by a series of balloon-borne experiments (Golden et al. 1979; Bogomolov et al. 1979; Bogomolov et al. 1987; Bogomolov et al. 1990; Hof et al. 1996; Mitchell et al. 1996; Moiseev et al. 1997; Yoshimura et al. 1995; Boezio et al. 1997; Matsunaga et al. 1998). The measurements are summarized in Table 1. The observed CR \bar{p}/p ratio has been shown to be in good agreement with predictions based on the Leaky Box Model (LBM) (Stephens 1981; Stephens & Golden 1987; Webber & Potgieter 1989; Gaisser & Schaefer 1992), which assumes that the \bar{p} 's originate from proton interactions in the interstellar (IS) medium. The \bar{p} 's then propagate within the Galaxy until they “leak out” with the characteristic CR Galactic storage time $T \sim 10$ million years (Myr)

(Webber et al. 1992; Chardonnet et al. 1996). If the \bar{p} lifetime $\tau_{\bar{p}}$ is not long compared to T the predicted \bar{p}/p spectrum will be modified. The agreement of the LBM predictions with the observed \bar{p}/p spectrum has therefore been used to argue that $\tau_{\bar{p}} > 10$ Myr (Golden et al. 1979; Bogomolov et al. 1979; Stephens 1981; Stephens & Golden 1987). This estimated limit is based on early CR \bar{p} data, and does not take into account the reduction of the \bar{p} decay rate due to time dilation, the effect of the heliosphere on the observed \bar{p}/p spectrum, or the systematic uncertainties associated with the predictions. In this paper we compare recent CR data with the predictions of an improved LBM extended to permit a finite $\tau_{\bar{p}}$. Heliospheric corrections and systematic uncertainties are taken into account. Assuming a stable \bar{p} , we find excellent agreement between our predictions and the CR observations. Allowing the \bar{p} to decay, we obtain a lower limit on $\tau_{\bar{p}}$ which is significantly more stringent than current laboratory bounds obtained from searches for \bar{p} decay in ion traps (Gabrielse et al. 1996) and storage rings (Geer et al. 1994; Hu et al. 1998). The analysis presented in this paper improves on our earlier analysis (Geer & Kennedy 1998) by including new data from Matsunaga et al. (1998).

CPT invariance requires $\tau_{\bar{p}} = \tau_p$, where the proton lifetime τ_p is known to exceed $\mathcal{O}(10^{32})$ yr (Caso et al. 1998). Although there is no compelling theoretical motivation to suspect a violation of CPT invariance, and hence a short \bar{p} lifetime, it should be noted that string theories can accommodate CPT violation. Consider a mass–dimension– n CPT–violating quantum field operator suppressed by the characteristic scale m_X , with $n > 4$. Dimensional analysis provides the estimate $m_p \tau_{\bar{p}} \sim [m_p/m_X]^{2n-8}$, yielding $m_X/m_p \sim [4.5 \times 10^{38} \cdot \tau_{\bar{p}}/10 \text{ Myr}]^{1/(2n-8)}$ (Kennedy 1999). For a given lower limit on $\tau_{\bar{p}}$, the implied lower limit on m_X is most stringent for $n = 5$. Note that if m_X is at the Planck scale ($1.2 \times 10^{19} \text{ GeV}/c^2$) and $n = 5$, the expected $\tau_{\bar{p}}$ would be ~ 10 Myr. Hence, a search for \bar{p} decay with a lifetime approaching 10 Myr provides a test for CPT violation well beyond the scale accessible at high energy colliders. Finally, since the antiproton is the only long lived antiparticle that could in principle decay into other known particles without violating charge conservation, a search for a modification of the CR \bar{p} spectrum due to \bar{p} decay provides a unique test of the stability of antimatter.

In the LBM the IS \bar{p} ’s are assumed to be produced by the interactions of CR p ’s (Stephens 1981; Stephens & Golden 1987; Webber & Potgieter 1989; Gaisser & Schaefer 1992): $pN_Z \rightarrow \bar{p}X$, where N_Z is a nucleus of charge Z , and X is anything. Our calculations use the elemental IS abundances given in Webber & Potgieter (1989) and Gaisser & Schaefer (1992), and the measured cross sections for $Z = 1$ (the dominant contribution) given in Stephens (1981). For $Z > 1$, we have used the “wounded nucleon” picture of Gaisser & Schaefer (1992). The \bar{p} ’s are assumed to propagate within the Galaxy until they are lost by either leakage into intergalactic space or by $p\bar{p}$ annihilation. The dominant loss process

is leakage. Our analysis is based on the LBM of Gaisser and Schaefer (1992), but with a Galactic storage time improved to account for the non-uniform Galactic CR distribution (Webber et al. 1992; Chardonnet et al. 1996). This *inhomogeneous leaky disk model* (ILDm) results in a momentum-dependent storage time $T(P) = (13 \text{ Myr}) [1 + P/(3 \text{ GeV})]^{-0.6}$.

The uncertainties on the parameters of the ILDM result in uncertainties on the normalization of the predicted \bar{p}/p ratio but, to a good approximation, do not introduce significant uncertainties in the shape of the predicted spectrum. Uncertainties on four ILDM parameters must be considered: (i) the storage time ($\pm 67\%$) (Webber et al. 1992), (ii) the IS primary p flux ($\pm 35\%$) (Gaisser & Schaefer 1992), (iii) the \bar{p} production cross section ($\pm 10\%$) (Stephens 1981; Gaisser & Schaefer 1992), and (iv) the composition of the IS medium, which introduces an uncertainty of $< 6\%$ on the predicted \bar{p} flux (Gaisser & Schaefer 1992). We neglect the last of these uncertainties since it is relatively small. Within the quoted fractional uncertainties on the other three parameters we treat all values as being a priori equally likely. Note that the predicted \bar{p}/p ratio is approximately proportional to each of the parameters under consideration.

The solid curves in Figure 1 show the ILDM \bar{p}/p spectra for the parameter choices that result in the largest and smallest \bar{p}/p predictions. The predicted IS spectrum does not give a good description of the observed distribution at the top of the atmosphere. Good agreement is not expected because the CR spectra observed at the Earth are modulated as the particles propagate into the heliosphere (Stix 1989; Encrenaz et al. 1990; Longair 1992), which consists of the solar magnetic field \mathbf{B} and the solar wind. The wind, which is assumed to blow radially outwards, has a measured equatorial speed $V_W \sim 400 \text{ km sec}^{-1}$. Away from the equatorial plane the *Ulysses* spacecraft has found $V_W \sim 750 \text{ km sec}^{-1}$ (Smith et al. 1995; Kóta & Jokipii 1995; Marsden et al. 1996; see also URL <http://ulysses.jpl.nasa.gov/>). The wind also carries the solar magnetic flux outward. Solar rotation Ω_\odot (Howard 1984) twists the field lines to form a Parker spiral. The smoothed heliomagnetic field ($B_\oplus \sim 5 \text{ nT}$ at the Earth’s orbit) declines as it changes from radial at the Sun to azimuthal in the outer Solar System. The heliomagnetic polarity ($\text{sign}(A)$) is opposite in northern and southern solar hemispheres and switches sign somewhat after sunspot maximum, roughly every 11 years. The regions of opposite magnetic polarity are separated by an approximately equatorial, unstable neutral current sheet. The sheet is wavy and spiraled; its waviness is measured by its “tilt” angle α , which relaxes from $\simeq 50^\circ$ at polarity reversal to $\lesssim 10^\circ$ just before reversal (Jokipii & Kopriva 1979; Encrenaz et al. 1990; Smith et al. 1995; Marsden et al. 1996; see also URL <http://www.nso.noao.edu/pub/sunspots>).¹ Cosmic rays enter the heliosphere on

¹The wavy sheet locus in polar co-ordinates is $\cos\theta + \sin\alpha \cdot \sin[\varphi + \Omega_\odot r/V_W] = 0$.

ballistic trajectories. The propagation of the CRs within the heliosphere is described by a drift–diffusion (Fokker–Planck) equation (Jokipii & Kopriva 1979; Risken 1984). The CRs are pushed outwards by the bulk motion of the wind (elastic scattering), lose energy as they perform work on the wind (adiabatic deceleration or inelastic scattering), are diffusively scattered by field turbulence, and execute a drift *orthogonal* to the curving magnetic field lines as they spiral inwards *along* the field lines. Particles with $qA > 0$ (< 0) drift in along a polar (sheet) route. The IS particles with sufficient energy to overcome the various energy losses reach the inner Solar System with degraded momenta.

We compute the modulation of the CR fluxes by the method of characteristics and combined Runge–Kutta/Richardson–Burlich–Stoer techniques (Zachmanoglou & Thoe 1976; Press et al. 1992). The calculation uses the heliospheric transport model of Jokipii & Kopriva (1979), Isenberg & Jokipii (1979, 1981), Jokipii & Thomas (1981), and Jokipii & Davila (1981) updated by *Pioneer*, *Voyager*, *Helios*, *IMP* and *Ulysses* heliospheric measurements (Smith et al. 1995; Marsden et al. 1996; see also URLs <http://nssdc.gsfc.nasa.gov/space/> and <http://www.sec.noaa.gov/>). Our calculation includes magnetic curvature drift since older heliospheric models that neglected this drift component (Gleeson & Axford 1967, 1968; Fisk & Axford 1969; Fisk 1971) have been shown to be inadequate (Isenberg & Jokipii 1979, 1981). The calculation is simplified by ignoring turbulence where its effects are small, which in practice means everywhere except across the sheet, where for particles with speed v the diffusion coefficient $\kappa_{\perp} = [(2 - 3) \times 10^{17} \text{ m}^2/\text{sec}][B_{\oplus}/B(r)](P/\text{GeV})^{0.3}(v/c)$ is used. The effects of diffusion away from the sheet are expected to become dominant for particles with kinetic energies < 300 MeV. In the following we restrict our analysis to the spectrum above 500 MeV to ensure that diffusion away from the sheet can be neglected.

We use the data sets recorded by the MASS91, IMAX, BESS, and CAPRICE experiments (Table 1). These data were recorded in the period 1991–1995, corresponding to a well–behaved part of the solar cycle for which the heliospheric modulation corrections can be confidently calculated. To explore the dependence of the predicted spectrum on the heliospheric parameters (equatorial V_W , polar V_W , and B_{\oplus}) we have computed the modulated spectra for 11 parameter sets (F1 – F11) that span the range of acceptable parameter values (Table 2). Using the central parameter values for our ILDM, and assuming a stable antiproton, the predicted modulated \bar{p}/p spectra for a fixed time in the solar cycle (July 1995) are shown in Figure 2 for each of the 11 heliospheric parameter sets. Figure 2 also shows the epoch–corrected measured CR spectra, obtained by multiplying each measurement by the factor $f \equiv R(\text{July 1995})/R(t)$, where $R(t)$ is the predicted \bar{p}/p ratio at time t . The factors f , which are shown in Table 1 and have been computed using the F6 parameters, vary by up to ± 0.06 with the parameter set choice. The predicted \bar{p}/p

spectra give an excellent description of the measurements. There is no evidence for an unstable \bar{p} .

To obtain a limit on $\tau_{\bar{p}}$ we add to the ILDM one additional loss mechanism, \bar{p} decay. The results from maximum likelihood fits to the measurements are shown in Figure 3 as a function of the assumed $\tau_{\bar{p}}$ for the 11 heliospheric parameter sets. The fits, which take account of the Poisson statistical fluctuations on the number of observed events and the background subtraction for each data set (Table 1), also allow the normalization of the ILDM predictions to vary within the acceptable range (Figure 1). For a stable \bar{p} , at the 95% C.L. all of the heliospheric parameter sets yield predictions that give reasonable descriptions of the observed \bar{p}/p spectrum. Allowing for a finite $\tau_{\bar{p}}$, the heliospheric parameter sets with larger wind speeds permit lower \bar{p} lifetimes. This can be understood by noting that, as the wind speed increases, the predicted flux of polar-routed particles (protons in the present solar cycle) is depleted at low energies, which increases the predicted \bar{p}/p ratio. Antiproton decay would compensate for this distortion in the predicted spectrum. Hence our fits using the extreme parameter set F11 determine the limits on $\tau_{\bar{p}}$. Under the assumption that there are no significant non-standard sources of cosmic ray antiprotons, we obtain the bounds:

$$\tau_{\bar{p}} > 0.8 \text{ Myr (90\% C.L.)} , \quad 0.7 \text{ Myr (95\% C.L.)} , \quad 0.5 \text{ Myr (99\% C.L.)} . \quad (1)$$

Our simple dimensional analysis suggests that if a dimension- n CPT-violating coupling results in antiproton decay, the mass scale m_X at which this new physics takes place exceeds $\mathcal{O}(10^{19}) \text{ GeV}/c^2$ ($\mathcal{O}(10^9) \text{ GeV}/c^2$), for $n = 5$ (6).

The limits (1) are significantly more stringent than those obtained from the most sensitive laboratory search for inclusive \bar{p} decay ($\tau_{\bar{p}} > 3.4$ months) (Gabrielse et al. 1996) or the most sensitive search for an exclusive \bar{p} decay mode ($\tau_{\bar{p}}/B(\bar{p} \rightarrow \mu^- \gamma) > 0.05 \text{ Myr}$) (Hu et al. 1998). Note however that these limits are less restrictive than the estimate $\tau_{\bar{p}} \gtrsim 10 \text{ Myr}$ given in Caso et al. (1998), which takes no account of systematic uncertainties or propagation effects and which is therefore overconstraining.

It is a pleasure to thank J. R. Jokipii (Lunar & Planetary Laboratory, Univ. Arizona) and E. J. Smith (Jet Propulsion Laboratory/CalTech) for their insights. This work was supported at Fermilab under grants U.S. DOE DE-AC02-76CH03000 and NASA NAG5-2788 and at the Univ. Florida, Institute for Fundamental Theory, under grant U.S. DOE DE-FG05-86-ER40272.

REFERENCES

- Boezio, M., et al. 1997, *ApJ*, 487, 415
- Bogomolov, E. A., et al. 1979, *Proc. 16th ICRC*, Kyoto, 1, 330
- Bogomolov, E. A., et al. 1987, *Proc. 20th ICRC*, Moscow, 2, 72
- Bogomolov, E. A., et al. 1990, *Proc. 21st ICRC*, Adelaide, 3, 288
- Caso, C., et al. (Particle Data Group) 1998, *Euro. Phys. J.*, C3, 613
- Chardonnet, P., et al. 1996, *Phys. Lett.*, B384, 161
- Encrenaz, T., et al. 1990, *The Solar System*, 2nd ed. (Berlin: Springer)
- Fisk, L. A., & Axford, W. I. 1969, *J. Geophys. Res.*, 74, 4973
- Fisk, L. A. 1971, *J. Geophys. Res.*, 76, 221
- Gabrielse, G., et al. (Antihydrogen Trap Collab.) 1996, CERN proposal CERN-SPSLC-96-23
- Gaisser, T. K., & Schaefer, R. K. 1992, *ApJ*, 394, 174
- Geer, S., et al. 1994, *Phys. Rev. Lett.*, 72, 1596
- Geer, S. H., & Kennedy, D. C. 1998, LANL preprint astro-ph/9809101
- Gleeson, L. J., & Axford, W. I. 1967, *ApJ*, 149, L115
- Gleeson, L. J., & Axford, W. I. 1968, *ApJ*, 154, 1011
- Golden, R. L., et al. 1979, *Phys. Rev. Lett.*, 43, 1196
- Hof, M., et al. 1996, *ApJ*, 467, L33
- Howard, R. 1984, *Ann. Rev. Astron. Astrophys.*, 22, 131
- Hu, M., et al. (APEX Collab.) 1998, *Phys. Rev.*, D58, 111101
- Isenberg, P. A., & Jokipii, J. R. 1979, *ApJ*, 234, 746
- Isenberg, P. A., & Jokipii, J. R. 1981, *ApJ*, 248, 845
- Jokipii, J. R., & Kopriva, D. A. 1979, *ApJ*, 234, 384
- Jokipii, J. R., & Thomas, B. 1981, *ApJ*, 243, 1115
- Jokipii, J. R., & Davila, J. M. 1981, *ApJ*, 248, 1156

- Kennedy, D. C. 1999, *Mod. Phys. Lett.*, A14, 849
- Kóta, J., & Jokipii, J. R. 1995, *Science*, 268, 1024
- Longair, M. S. 1992, *High Energy Astrophysics*, 2 vols., 2nd ed. (Cambridge: Cambridge University Press)
- Marsden, R. G., et al. 1996, *Astron. Astrophys.*, 316, 279ff
- Matsunaga, H., et al. 1998, *Phys. Rev. Lett.*, 81, 4052
- Mitchell, J. W., et al. 1996, *Phys. Rev. Lett.*, 76, 3057
- Moiseev, A., et al. 1997, *ApJ*, 474, 479
- Press, W. H., et al. 1992, *Numerical Recipes in C: The Art of Scientific Computing*, 2nd ed. (Cambridge: Cambridge University Press)
- Risken, H. 1984, *The Fokker–Planck Equation: Methods of Solution and Applications* (New York: Springer).
- Smith, E. J., et al. 1995, *Science*, 268, 1005ff
- Stephens, S. A. 1981, *Astrophys. Space Sci.*, 76, 87
- Stephens, S. A., & Golden, R. L. 1987, *Space Sci. Rev.*, 46, 31
- Stix, M. 1989, *The Sun: An Introduction* (Berlin: Springer)
- Webber, W. R., & Potgieter, M. S. 1989, *ApJ*, 344, 779
- Webber, W. R., et al. 1992, *ApJ*, 390, 96
- Yoshimura, K., et al. 1995, *Phys. Rev. Lett.*, 75, 3792
- Zachmanoglou, E. C., & Thoe, D. .W. 1976, *Introduction to Partial Differential Equations with Applications* (reprint; New York: Dover, 1986)

Table 1: Summary of Cosmic Ray Antiproton Results

Experiment	Field Pol. ^a	Flight Date	f^b	KE Range (GeV)	Cand- idates	Back- ground	Observed \bar{p}/p Ratio	Predict- tion ^c
Golden et al. 1979 [†]	+	June 1979	–	5.6 – 12.5	46	18.3	$(5.2 \pm 1.5) \times 10^{-4}$	–
Bogomolov et al. 1979 [†]	+	1972-1977	–	2.0 – 5.0	2	–	$(6 \pm 4) \times 10^{-4}$	–
Bogomolov et al. 1987 [‡]	–	1984-1985	–	0.2 – 2.0	1	–	$(6_{-5}^{+14}) \times 10^{-5}$	–
Bogomolov et al. 1990 [‡]	–	1986-1988	–	2.0 – 5.0	3	–	$(2.4_{-1.3}^{+2.4}) \times 10^{-4}$	–
MASS91 ^d	+	Sep. 1991	1.1	3.70–19.08	11	3.3	$(1.24_{-0.51}^{+0.68}) \times 10^{-4}$	1.3×10^{-4}
IMAX ^{e‡}	+	July 1992	–	0.25 – 1.0	3	0.3	$(3.14_{-1.9}^{+3.4}) \times 10^{-5}$	1.5×10^{-5}
IMAX ^e	+	July 1992	0.96	1.0 – 2.6	8	1.9	$(5.36_{-2.4}^{+3.5}) \times 10^{-5}$	6.5×10^{-5}
IMAX ^e	+	July 1992	1.1	2.6 – 3.2	5	1.2	$(1.94_{-1.1}^{+1.8}) \times 10^{-4}$	1.1×10^{-4}
BESS93 ^{f‡}	+	July 1993	–	0.20 – 0.60	7	~ 1.4	$(5.2_{-2.8}^{+4.4}) \times 10^{-6}$	8.9×10^{-6}
CAPRICE ^g	+	Aug. 1994	0.94	0.6 – 2.0	4	1.5	$(2.5_{-1.9}^{+3.2}) \times 10^{-5}$	3.5×10^{-5}
CAPRICE ^g	+	Aug. 1994	1.0	2.0 – 3.2	5	1.3	$(1.9_{-1.0}^{+1.6}) \times 10^{-4}$	1.1×10^{-4}
BESS95 ^{h‡*}	+	July 1995	1.0	0.175 – 0.3	3	0.17	$(7.8_{-4.8}^{+8.3}) \times 10^{-6}$	–
BESS95 ^{h‡*}	+	July 1995	1.0	0.3 – 0.5	7	0.78	$(7.4_{-3.3}^{+4.7}) \times 10^{-6}$	1.1×10^{-5}
BESS95 ^{h*}	+	July 1995	1.0	0.5 – 0.7	7	1.4	$(7.7_{-3.7}^{+5.3}) \times 10^{-6}$	5.5×10^{-6}
BESS95 ^{h*}	+	July 1995	1.0	0.7 – 1.0	11	2.8	$(1.01_{-4.3}^{+5.7}) \times 10^{-5}$	1.3×10^{-5}
BESS95 ^{h*}	+	July 1995	1.0	1.0 – 1.4	15	3.5	$(1.99_{-0.73}^{+0.91}) \times 10^{-5}$	3.1×10^{-5}

^a Heliomagnetic field polarity.

^b Epoch correction factor; see text.

^c ILDM prediction using F6 heliospheric parameters; see text.

^d Hof et al. 1996. ^e Mitchell et al. 1996. ^f Moiseev et al. 1997. ^g Boezio et al. 1997.

^h Matsunaga et al. 1998.

[†] Not shown in Fig. 1 or used in analysis. [‡] Not used in analysis. ^{*} Statistical and systematic uncertainties on ratio added in quadrature.

Table 2: Heliospheric Parameter Sets

Set	Equatorial V_W (km sec ⁻¹)	Polar V_W (km sec ⁻¹)	B_\oplus (nT)
F1	375	700	4.0
F2	380	710	4.1
F3	385	720	4.2
F4	390	730	4.3
F5	395	740	4.4
F6	400	750	4.5
F7	405	760	4.6
F8	410	770	4.7
F9	415	780	4.8
F10	420	790	4.9
F11	425	800	5.0

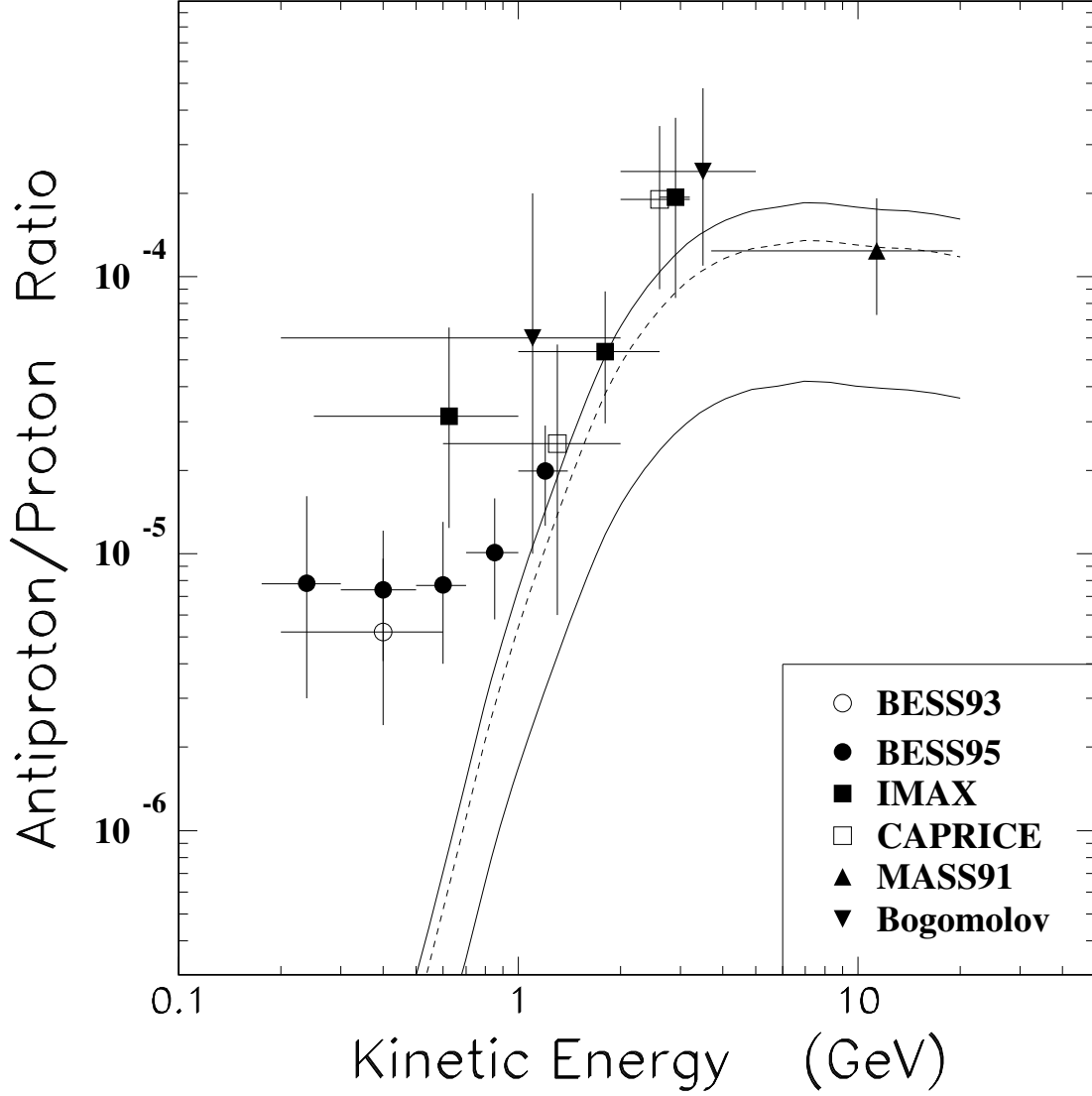


Fig. 1.— Observed \bar{p}/p ratio at the top of Earth atmosphere (see Table 1). The solid curves show the upper and lower interstellar ratios predicted by the ILDM described in the text, without solar modulation. The broken curve shows the ILDM prediction with the same parameters used for the modulated predictions of Fig. 2.

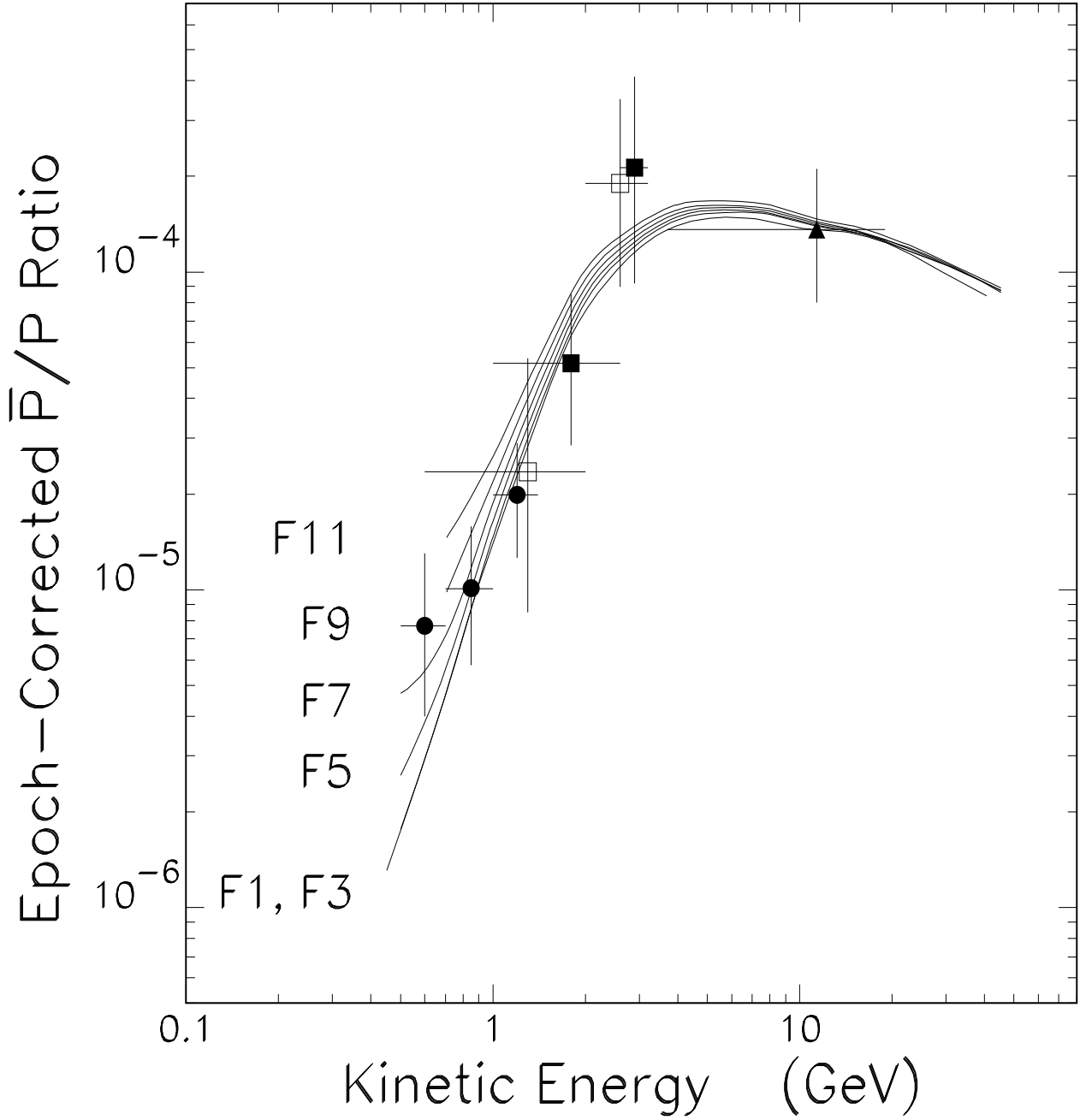


Fig. 2.— Observed \bar{p}/p spectrum (kinetic energy > 500 MeV) at the top of the atmosphere compared with the ILDM predictions (see broken curve on Fig. 1) after modulation using the heliospheric parameter sets indicated (see Table 2). The curves are predictions for the spectrum observed in July 1995. The data have been corrected to correspond to this epoch (see text).

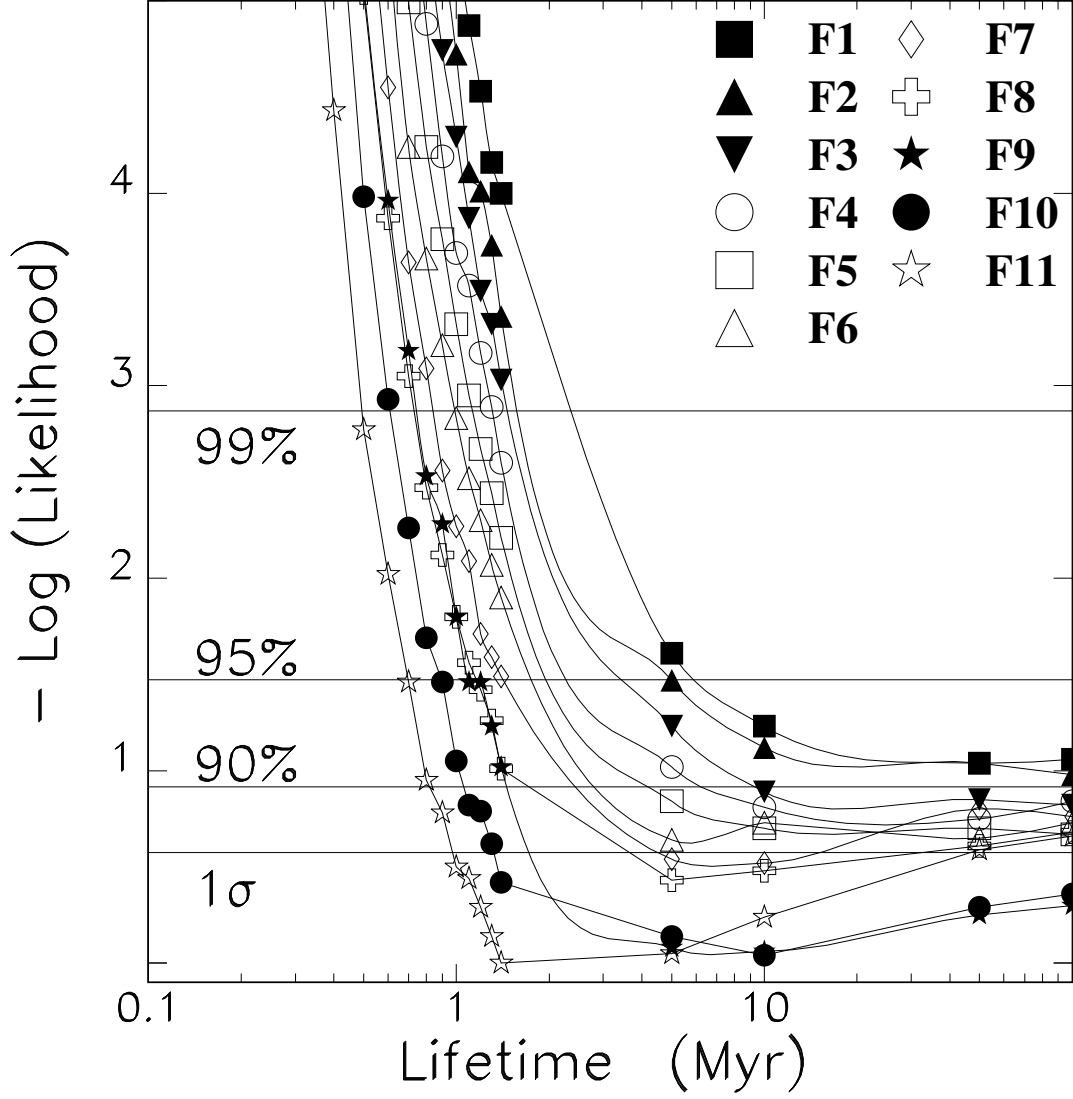


Fig. 3.— Fit results as a function of the assumed $\tau_{\bar{p}}$ for the eleven heliospheric parameter sets (F1 – F11) shown in Table 2.